JOURNAL OF MATERIALS SCIENCE 29 (1994) 2459–2466

# Synthesis of large pore-size and large pore-volume aluminas by glycothermal treatment of aluminium alkoxide and subsequent calcination

M. INOUE, H. KOMINAMI, T. INUI
*Department of Hydrocarbon Chemistry, Faculty of Engineering, Kyoto University, Yoshida, Kyoto 606-01, Japan*

Aluminas were prepared by calcination of the products obtained by glycothermal treatment of aluminium alkoxides, and their pore structures investigated by means of the nitrogen adsorption technique and mercury porosimetry. The product had a honeycomb-like texture which developed well with increasing crystallite size of the product. The crystallite size of the product was in turn controlled by the glycol used, and increased in the following order (carbon number of glycol): $2 < 3 < 6 \ll 4$. The honeycomb-like texture was preserved even after calcination. Because of the well-developed honeycomb-like texture, the alumina derived from the product obtained by the treatment of aluminium isopropoxide in 1,4-butanediol had quite large pore diameters (70 and 700 nm) and a large pore volume (2.4 $cm^3 g^{-1}$) with a sufficient surface area (184 $m^2 g^{-1}$).

## 1. Introduction

Alumina is most widely used for supports of industrial catalysts; it is inexpensive, reasonably stable and can be provided with a wide range of surface areas and porosities suitable for a variety of catalytic applications [1]. To avoid diffusion problems, large pore-size aluminas are usually favoured in industrial processes. For example, in hydrotreatment of heavy oil, shale oil, tar sand liquid or coal liquid, the catalyst with a larger pore-size showed a better performance than that with a smaller pore-size, despite having a smaller surface area [2, 3]. This is explained by the ease of diffusion of large molecular-weight reactant molecules in larger pores. Moreover, when catalysts with small pores are used in this reaction, metals such as V and Ni are deposited at the entrance of the pores, and finally metal particles blockade the pores. This completely destroys catalyst activity, even though the core of the catalyst is still active; this phenomenon is known as 'pore mouth plugging' [4].

For a mass of agglomerate composed of the closest packing of spherical particles, specific surface area ($S$) and mean pore radius ($\bar{r}$) are given by the following equations:

$$S = \frac{3}{\rho a} \quad (1)$$

$$\bar{r} = \left(\frac{2(2)^{1/2}}{\pi} - \frac{2}{3}\right)a \quad (2)$$

where $a$ and $\rho$ are the radius and density of the particles, respectively. Obviously, with an increasing radius of the particles, the pore size becomes larger. However, at the same time the specific surface area decreases, which is undesirable for most catalyst uses. To solve this dilemma, several techniques have been developed [5–11]. One method is to form micropores within the large particles [5–10]. Calcination of well crystallized aluminium hydroxides or oxyhydroxides forms intraparticle pores within the pseudomorph of the original crystal of the hydroxides or oxyhydroxides. In another method, combustible materials such as fibre and carbon black are mixed with an alumina source such as pseudoboehmite (microcrystalline boehmite) and the admixture is pelleted and then fired [11]. In addition to the mesopores developed between alumina particles, macropores are formed after combustion of the admixed materials. However, macropores formed in this way are not always open to the outside of the pellet, and therefore only small portions of the macropores may be effective. Moreover, when the proportion of the macropore is increased by the increased amount of combustible material, the mechanical strength of the pellet drastically decreases.

If primary particles are irregular in shape, the above-mentioned relation does not hold any more. This problem may be overcome by making primary particles as irregular as possible. During the course of a long-term study on controlling the pore texture of alumina support [12–15], it has been found that the thermal treatment of crystalline aluminium hydroxide (gibbsite) in a glycol medium (glycothermal treatment of gibbsite) yielded a novel derivative of boehmite, in which the glycol moieties were incorporated into the boehmite layers [14]. In a subsequent paper [15], it was reported that the glycothermal treatment of

0022–2461  

aluminium alkoxides also yielded the glycol derivative of boehmite.

In the present paper, the pore texture of aluminas prepared by calcination of the products obtained by glycothermal treatment of aluminium alkoxide is reported.

## 2. Experimental procedure

### 2.1. Glycothermal treatment of aluminium alkoxide

A suspension of 12.5 g aluminium triisopropoxide (AIP) in 130 $cm^3$ of a glycol [ethylene glycol (EG), 1,3-propanediol (PG), 1,4-butanediol (BG), or 1,6-hexanediol (HG)] was placed in a test tube, which was then set in a 300 $cm^3$ autoclave. An additional 30 $cm^3$ of the glycol was placed in the gap between the autoclave wall and the test tube. After the atmosphere inside the autoclave was thoroughly replaced with nitrogen, the mixture was heated to the desired temperature (250–300 °C) at a rate of 2.3 °C $min^{-1}$ and held at that temperature for 2 h under the spontaneous vapour pressure of the glycol. After the mixture had been cooled, the resulting precipitates were washed with methanol by repeated cycles of centrifugation and decantation, and then air-dried. The product was fine white powders, and was stable in wet atmosphere.

### 2.2. Calcination

Two series of experiments were carried out. In one series, the samples obtained by glycothermal treatment were pre-dried at 130 °C for 2 h, then calcined at 600 °C for 2 h in a box furnace. In the other series, pre-dried samples were heated at the rate of 2.5 °C $min^{-1}$ in a tubular furnace under a 40 $dm^3$ $min^{-1}$ air flow. During the course of heating, small portions were taken out from each sample at the desired temperatures and the rest was further heated. Thus alumina samples calcined at up to 1200 °C were obtained. The calcined samples were kept in a desiccator or in sealed ampoules. These aluminas will be designated by the abbreviations for the media used in glycothermal treatment, followed by the calcination temperatures in degrees Celsius in parentheses. The original samples from the glycothermal treatment will be specified by the term "as syn" in parentheses.

### 2.3. Characterization

X-ray diffraction (XRD) was measured on a Rigaku Geigerflex-2013 diffractometer employing Cu$K\alpha$ radiation and an Ni filter. Nitrogen adsorption isotherms were measured on a Micromeritics AccuSorb 2100E instrument at 77.4 K employing the conventional constant-volume method. Isotherms and surface areas were quoted for 1 g of outgassed solid without correction for the water or organic moiety remaining after outgassing at 180 °C for 2 h for the calcined aluminas, or at room temperature for 9 h following to drying at 130 °C for 2 h for the products. Surface areas were calculated by applying the usual BET procedure to the adsorption data, taking the average area occupied by a nitrogen molecule as 0.162 $nm^2$.

Pore size distribution curves in the range 3–30 nm were calculated from the nitrogen adsorption isotherms by the Cranston–Inkley method [16] and those in the range larger than 30 nm were determined by a mercury porosimeter, Micromeritics Auto-pore 9200.

The morphology of the products was observed with a scanning electron microscope (SEM), Hitachi-Akashi MSM-102.

## 3. Results and discussion

### 3.1. General features of the glycothermal treatment of AIP

As the pore textures of the products obtained by glycothermal treatment of AIP and of the derived alumina are closely related to the reaction paths, general features of the reaction will be briefly described in this section. As discussed in a previous paper [15], glycothermal treatment of aluminium alkoxide at 300 °C yielded the glycol derivatives of boehmite, the structure of which was identical to that of the product obtained by the glycothermal treatment of gibbsite [14]. Some properties of the products obtained by the glycothermal treatment of AIP in various

TABLE I Properties of the products obtained by the glycothermal treatment of aluminium isopropoxide in glycols at 300 °C for 2 h

| Properties | Ethylene glycol | 1,3-Propanediol | 1,4-Butanediol | 1,6-Hexanediol |
|---|---|---|---|---|
| Glycol/Al | 0.57 | 0.37 | 0.26 | 0.22 |
| Crystallite size[a] (nm) | 5 | 11 | 29 | 13 |
| Surface area ($m^2$ $g^{-1}$) | 516 | 223 | 150 | n.d. |
| Ignition loss (%) | 39.5 | 31.7 | 37.8 | 36.7 |
| Bulk density | 0.28 | 0.19 | 0.14 | 0.42 |
| Pore volume ($cm^3$ $g^{-1}$) | | | | |
| ($D < 30$ nm) | 0.69 | 0.86 | 0.41 | n.d. |
| ($D > 30$ nm) | 1.58 | 2.52 | 1.43 | 0.66 |
| Total | 2.27 | 3.38 | 1.83 | n.d. |
| Mode pore diameter (nm) | | | | |
| mesopore region | 4 | 20 | 100 | n.d. |
| macropore region | – | 1000 | 1000 | n.d. |

[a] Calculated by the Scherrer equation; shape factor, $K$, taken as 1.84.

glycols at 300 °C are given in Table I. The crystallite size of the product calculated from the half-height width of the 020 diffraction peak varied with the carbon number of glycol and increased in the following order:

$$2 < 3 < 6 \ll 4 \text{ (carbon number of glycol).}$$

The amount of glycol moieties remaining in the product decreased with increasing crystallite size (growth of layers) of the product, suggesting that the cleavage of the glycol moiety was the key factor controlling crystallite size. As the order mentioned above agreed with the order of the solvolysis rate of ω-methoxyalkyl *p*-bromobenzenesulphonate ($CH_3O(CH_2)_nOBs$) [17], it was concluded that heterolytic cleavage of the C–O bonds of $HO(CH_2)_n$–O–Al <, formed by alkoxide exchange between aluminium alkoxide and glycol, controlled the development of the boehmite layer structure. In the case of BG, the cleavage of the C–O bond was accelerated by the intramolecular participation of the hydroxyl group, as depicted below:

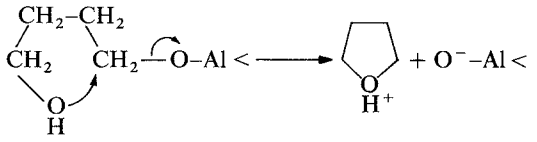

A honeycomb-like texture (Fig. 1), as observed in the product obtained by the glycothermal treatment of gibbsite [14], was also seen in the product, and the texture developed well with the increase in crystallite size of the product.

## 3.2. Pore structure of the products obtained by glycothermal treatment of AIP in various glycols

Nitrogen adsorption isotherms of the products are shown in Fig. 2a. De Boer [18] classified the shapes of hysteresis loops of adsorption–desorption isotherms into five categories. According to his classification, the isotherms of PG(as syn) and BG(as syn) belong to the E-type hysteresis, which is explained either by pores with an ink-bottle shape, or by pores having varying

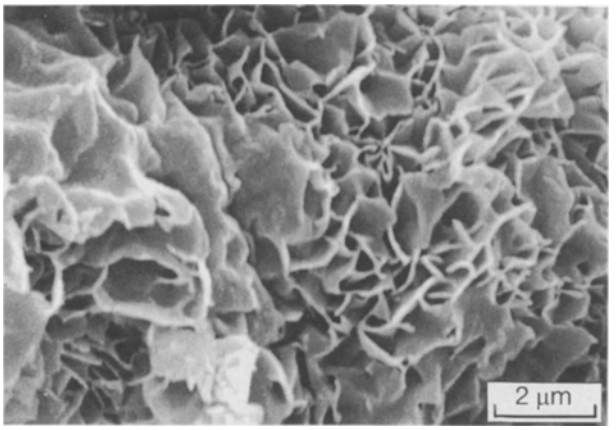


*Figure 1* Scanning electron micrograph of the product obtained by glycothermal treatment of aluminium isopropoxide in 1,4-butanediol at 300 °C for 2 h.

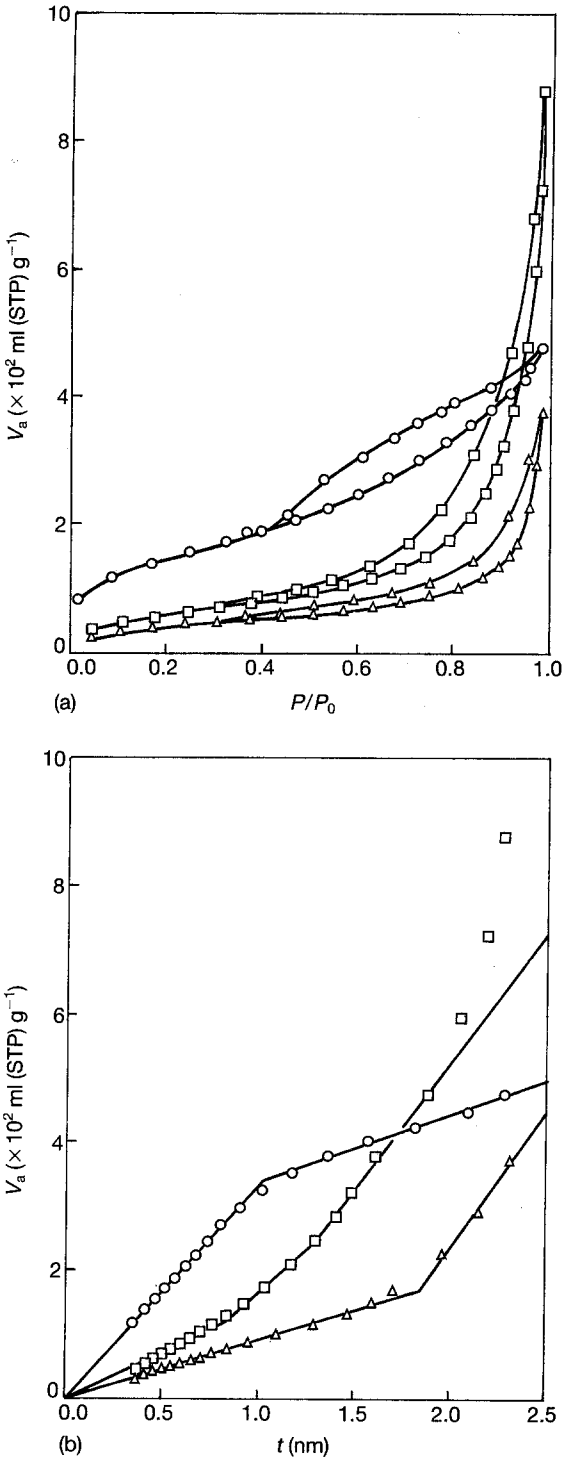


*Figure 2* Nitrogen adsorption isotherms (a) and *t*-plots (b) of the products obtained by glycothermal treatment of aluminium isopropoxide in various glycols at 300 °C for 2 h. ○, Ethylene glycol; □, 1,3-propanediol; △, 1,4-butanediol.

widths. For the present samples, the latter explanation seems to be more feasible as the pores formed between primary particles have varying widths. The hysteresis loop of EG(as syn) appears to belong to the B-type, explained by slit-shaped capillaries with parallel walls. As the boehmite layer structure of EG(as syn) was only poorly developed, slit-shaped micropores may have been formed between small plate-like crystals of the glycol derivative of boehmite.

More information can be obtained from Lippens–de Boer's *t*-plot [19, 20] (Fig. 2b). In the *t*-plot, the *x*

and $y$ coordinates are the statistical thickness of the nitrogen layer adsorbed on non-porous solids and the amount of nitrogen adsorbed on the products, respectively. Lippens & de Boer [20] classified the shapes of $t$-plot into three types. When a sample has neither micro- nor mesopores, the $t$-plot exhibits a straight line going through the origin. When a sample has micropores, the slope of the $t$-plot decreases abruptly after micropores are filled with adsorbate molecules. When a sample has mesopores, the slope of the $t$-plot increases because of capillary condensation of adsorbate molecules into mesopores.

The $t$-plot of EG(as syn) showed a decrease in slope due to the micropore filling [20]. The slope of the $t$-plots of PG(as syn) and BG(as syn) increased, indicating that both samples had mesopores. As capillary condensation in BG(as syn) began at a larger $t$ value, BG(as syn) had larger mesopores than PG(as syn), which is further confirmed by the pore size distribution curves shown in Fig. 3. In the mesopore region, the curves of EG(as syn), PG(as syn) and BG(as syn) had peaks at 4, 20 and 100 nm, respectively. Therefore the mode pore diameter of the product increased with increasing crystallite size (the primary particle size). As discussed from the hysteresis loop, these pores were formed between primary particles. Therefore the mode pore diameter reflects the primary particle size.

The mode pore diameter of EG(as syn) was larger than expected from the $t$-plot. However, the pore size distribution curves are derived from differentiation of the plots for the cumulative pore volume against the logarithm of the pore diameter. The population of wider pores is always exaggerated by this type of distribution curve, and the curve for the surface area distribution of EG(as syn) against the pore diameter exhibited a peak at 2 nm (lower limit of the pore diameter which can be determined by the nitrogen adsorption method).

As seen in Fig. 3, PG(as syn) and BG(as syn) had a bimodal pore distribution and a distribution peak at $\sim 1000$ nm, in addition to the peaks at the mesopore region. The macropores can be attributed to the voids of the honeycomb-like texture shown in Fig. 1. The absence of macropores of EG(as syn) is attributed to the lack of the honeycomb-like texture.

The BET surface area and the bulk density of the product decreased with increasing crystallite size of the product (Table I). Generally, the bulk density of powder materials increases with an increase in particle size (or a decrease in the surface area). Nevertheless, the bulk densities of the present products show a tendency contrary to the general rule. This is explained as follows: with the increase in crystallite size of the product, the surface area decreased, while the honeycomb-like texture developed well. The honeycomb-like texture possessed large voids (macropores) and because of these voids, the product with a large crystallite size (a lower surface area) had a low bulk density.

### 3.3. Pore structure of aluminas prepared by calcination of glycothermal treatment products at 600 °C

The products were calcined at 600 °C and the pore texture of the resulting alumina was examined. Nitrogen adsorption isotherms and $t$-plots of the aluminas are shown in Fig. 4a and b, respectively. The $t$-plot of EG(600) showed an increase in slope due to capillary condensation into mesopores, and then a decrease in slope due to mesopores being filled with nitrogen. This suggests that the pore size was distributed in a narrow range, which is actually shown by the pore size distribution curve (Fig. 5). However, the $t$-plot of EG(600) did not show any sign of the presence of micropores. Because EG(as syn) had a small crystal-

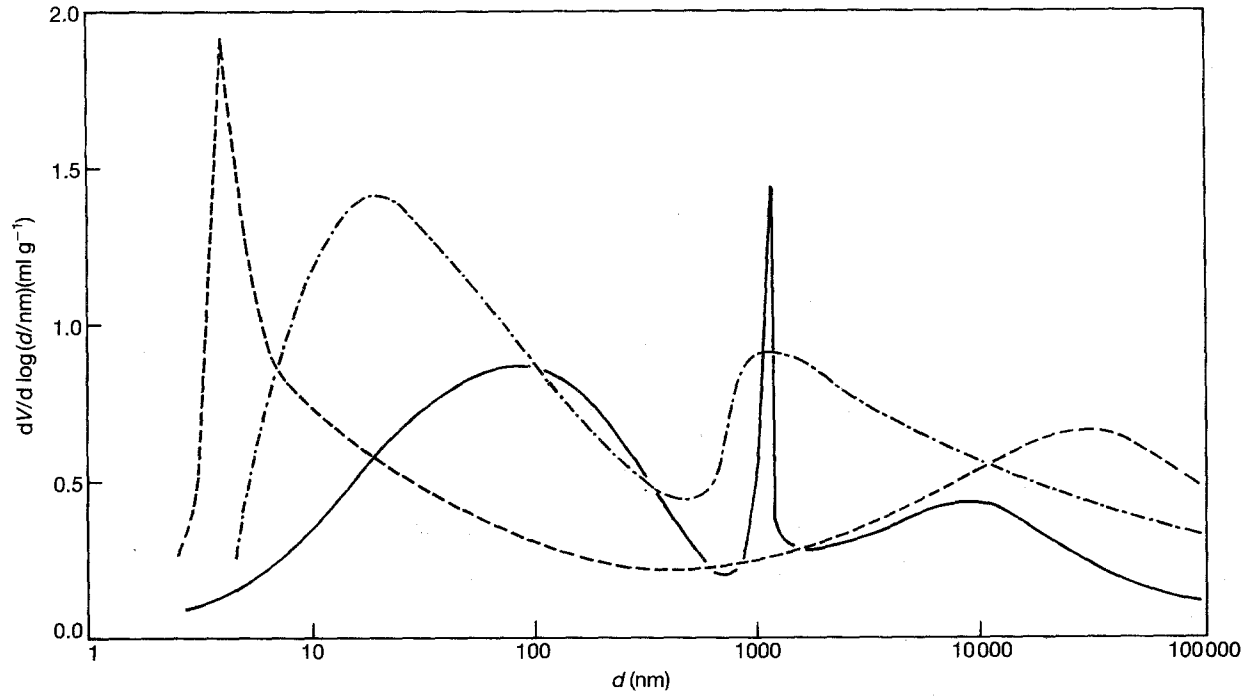


*Figure 3* Pore size distribution curves of the products. (– – – –) Ethylene glycol; (– – – – – –) 1,3-propanediol; (———) 1,4-butanediol.

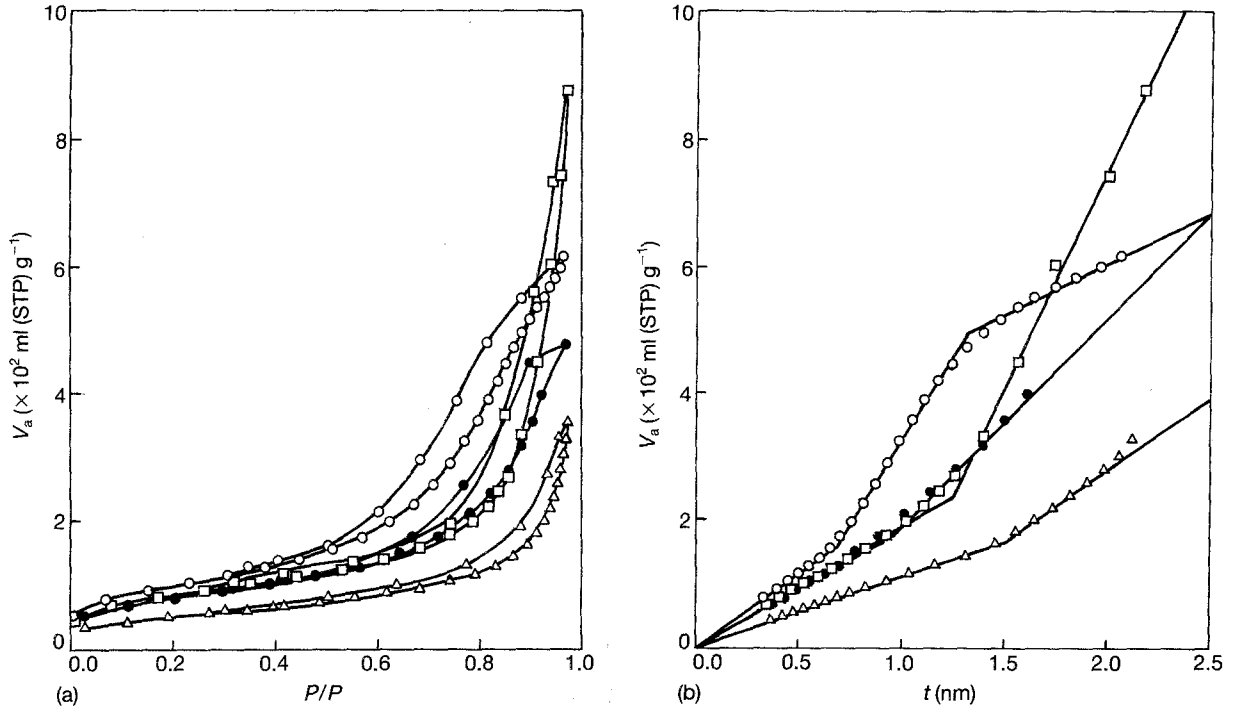


*Figure 4* Nitrogen adsorption isotherms (a) and $t$-plots (b) of aluminas prepared by calcination of glycothermal products at 600 °C. ○, Ethylene glycol; □, 1,3-propanediol; △, 1,4-butanediol; ●, 1,6-hexanediol.

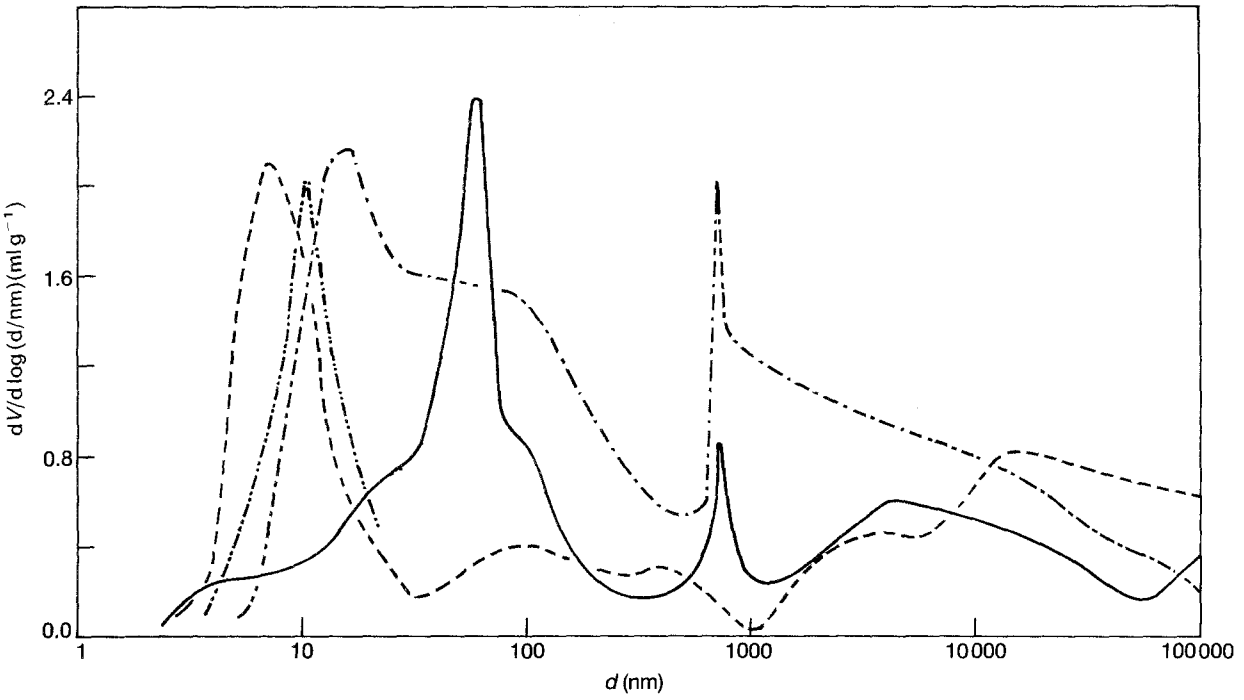


*Figure 5* Pore size distribution curves of the aluminas. (——) Ethylene glycol; (– – – –) 1,3-propanediol; (———) 1,4-butanediol; (– – – – – –) 1,6-hexanediol.

lite size, the primary particles possessed a large surface energy, and therefore had a good ability for sintering the particles. Calcination of EG(as syn) resulted in a large decrease in surface area (Table II). Sintering the primary particles diminished the micropores formed between primary particles, and the average diameter of the resulting void was enlarged.

The slope of the $t$-plot of BG(600) slightly decreased at around $t = 0.8$ nm and increased at around $t = 1.5$ nm, suggesting that BG(600) had both micro- and mesopores. It is well known that calcination of well-crystallized boehmite (crystallite size $> 10$ nm) affords alumina with micropores inside the pseudomorph of the boehmite particles [10, 20] whereas microcrystalline boehmite (crystallite size $< 10$ nm) does not create micropores on calcination [20–22]. The crystallite size of the glycol derivative of boehmite in BG(as syn) was sufficiently large (29 nm), and there-

TABLE II Properties of aluminas prepared by calcination of the glycothermal products at 600 °C[a]

| Properties | Ethylene glycol | 1,3-Propanediol | 1,4-Butanediol | 1,6-Hexanediol |
|---|---|---|---|---|
| Surface area ($m^2 g^{-1}$) | 354 | 297 | 184 | 284 |
| Bulk density | 0.23 | 0.15 | 0.13 | n.d. |
| Pore volume ($cm^3 g^{-1}$) | | | | |
| ($D < 30$ nm) | 1.00 | 1.06 | 0.43 | 0.77 |
| ($D > 30$ nm) | 1.76 | 3.67 | 1.97 | n.d. |
| Total | 2.76 | 4.73 | 2.40 | n.d. |
| Mode pore diameter (nm) | | | | |
| mesopore region | 7 | 16 | 70 | 11 |
| macropore region | – | 700 | 700 | n.d. |

[a] Glycothermal treatment conditions as described in Table I.

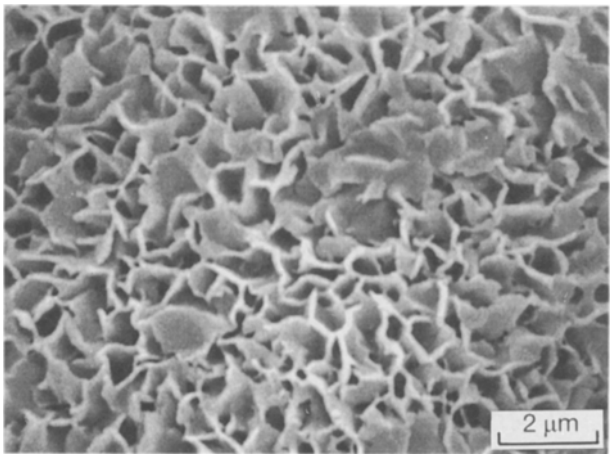


*Figure 6* Scanning electron micrograph of the alumina (BG(600)) prepared by calcination of BG(as syn) at 600 °C.

fore micropores seem to have been formed inside the particles as water molecules and glycol moieties were expelled from the particles to form an alumina lattice. However, the surface area calculated from the slope of the second segment of the *t*-plot after all the micropores were filled with nitrogen was 164 $m^2 g^{-1}$, which means that the surface area due to micropores was about 20 $m^2 g^{-1}$, only 10% of the total surface area (184 $m^2 g^{-1}$).

The *t*-plots of PG(600) and HG(600) also showed an increase in slope, which indicates that these aluminas also had mesopores. In agreement with these results, the pore size distribution curves of EG(600), PG(600), BG(600) and HG(600) exhibited peaks at around 7, 16, 70 and 11 nm, respectively (Fig. 5 and Table II). The mode pore diameter of the calcined alumina increased with increasing crystallite size of the originating sample.

In addition to the peak at the mesopore region, the distribution curves of PG(600) and BG(600) exhibited a peak at 700 nm. Because the honeycomb-like texture was preserved even after calcination (Fig. 6), these mesopores can be explained by this texture.

When pore structures of the product and the alumina obtained by calcination of the product are compared, the mode pore diameters of all the aluminas except EG(600) were smaller than those of the corresponding products. Judging from the BET surface area of the alumina, sintering of the primary particles took place to a negligible extent during calcination. This is attributed to the fairly large crystallite size of PG(as syn), BG(as syn) and HG(as syn). Because the formation of alumina from the glycol derivative of boehmite is accompanied by a large decrease in crystallographic specific gravity, each primary particle must have shrunk during calcination. Because mesopores were formed in the voids between primary particles, shrinkage of the primary particles resulted in a decrease in the mode pore diameter. As the honeycomb-like texture is formed by the crystals (not crystallite) of the glycol derivative of boehmite, calcination also caused shrinkage of the texture, resulting in a decrease in the mode pore diameter in the macropore region.

Some properties of the aluminas are given in Table II. In all the aluminas, pore volumes increased on calcination; a part of this increase is attributed to the weight loss per unit volume. The relationship between bulk density and surface area of alumina was also opposite to the general tendency. The bulk density of BG(600) was $\sim 0.13$, which is much lower than for commercial aluminas (usually $> 0.4$). It must be noted that BG(600), having the smallest surface area of the aluminas prepared here, still had a sufficient surface area (184 $m^2 g^{-1}$) with large mode pore diameters (70 nm and 700 nm) and large pore volume (2.4 $cm^3 g^{-1}$), because of the well-developed honeycomb-like texture.

## 3.4. Effect of calcination temperature

The product obtained by glycothermal treatment of AIP in PG at 300 °C was calcined at various temperatures, and the effect of calcination temperature on the pore texture of the resulting alumina was examined. The XRD patterns of the product and the aluminas are shown in Fig. 7. PG(600) was amorphous to X-ray. γ-Alumina was formed when the temperature was raised to 1000 °C. θ-Alumina appeared at around 1100 °C, and at 1200 °C, α-alumina was formed; however, θ-alumina remained.

The *t*-plots of the aluminas are shown in Fig. 8. Each plot exhibited an increase in slope, and the point of intersection of the two segments shifted toward a large *t* value with elevation of the calcination temperature. As explained above, calcination of the product

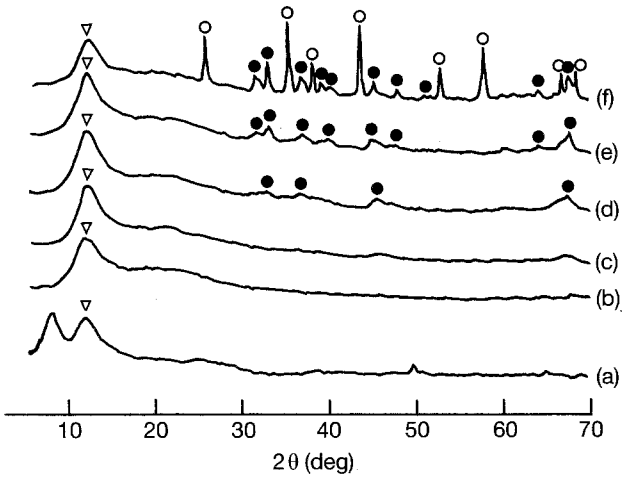


*Figure 7* XRD patterns of (a) glycothermal product obtained in 1,3-propanediol; (b–f) aluminas prepared by calcination of the product at 600, 800, 1000, 1100 and 1200 °C, respectively. The broad peak at $2\theta = 11.5°$, indicated by ▽, is due to grease used to mount the sample, and peaks, indicated by (●) and (○), are assigned to transition alumina (γ and/or θ phase) and α-alumina, respectively.

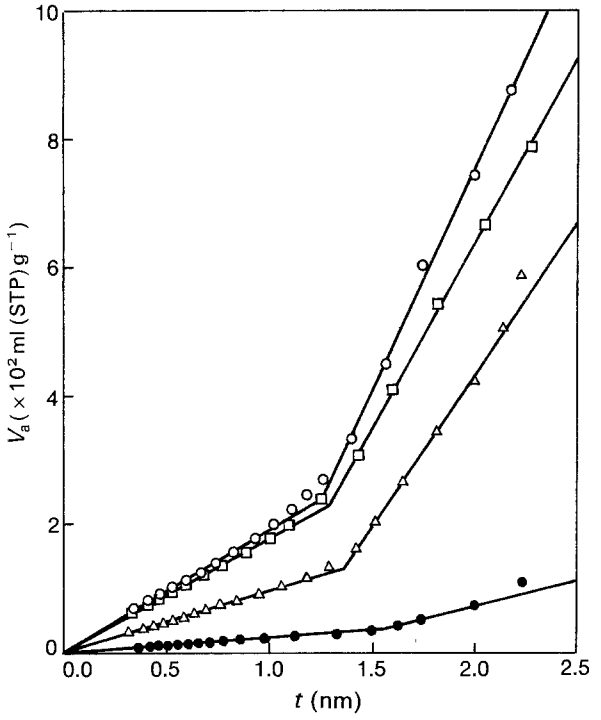


*Figure 8* Effect of calcination temperature of the glycothermal product obtained in 1,3-propanediol upon the pore structure of the resulting aluminas. ○, 600; □, 800; △, 1000, ●, 1200 °C.

at 600 °C decreased the mode pore diameter, while further calcination enlarged the mode pore diameter (Table III). This enlargement of the mode pore diameter is explained by sintering of the primary particles, because the surface area of alumina decreased with a rise in calcination temperature. Mesopores have almost disappeared in PG(1200); however, SEM photographs (Fig. 9) showed that the honeycomb-like texture was preserved even in PG(1200). Consistent with these results, PG(1200) had a relatively large surface area (37 $m^2 g^{-1}$) and a relatively small bulk density (0.30), suggesting that sintering of the alumina particles proceeded slowly, even at 1200 °C.

## 4. Conclusions

Calcination of the products obtained by glycothermal treatment of aluminium alkoxide yielded aluminas with a honeycomb-like texture. The honeycomb-like texture developed well in the following order: (carbon number of glycol) $2 < 3 < 6 \ll 4$, which was in the same order for the crystallite size of the uncalcined product. When 1,4-butanediol was used as the medium for the glycothermal treatment, alumina with quite large mode pore diameters (70 and 700 nm) and a large pore volume (2.4 $cm^3 g^{-1}$), with a sufficient surface area (184 $m^2 g^{-1}$) was obtained. Therefore

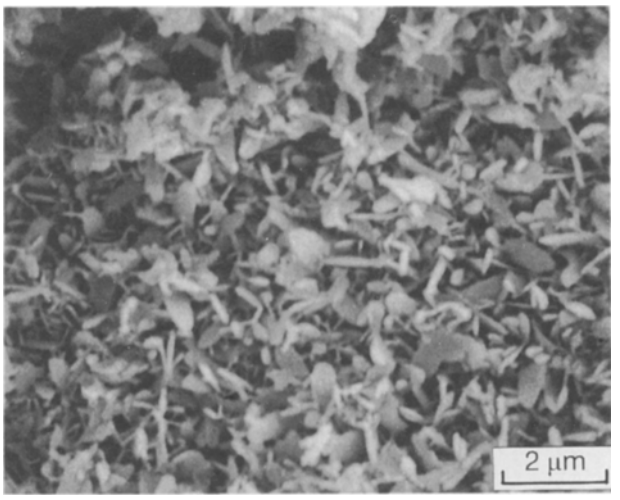


*Figure 9* Scanning electron micrograph of the alumina (PG(1200)) prepared by calcination of PG(as syn) at 1200 °C.

TABLE III Properties of aluminas prepared by calcination of the product obtained by glycothermal treatment in 1,3-propanediol[a]

| Properties | Glycothermal product | Calcination temperature (°C) | | | |
|---|---|---|---|---|---|
| | | 600 | 800 | 1000 | 1200 |
| Surface area ($m^2 g^{-1}$) | 223 | 297 | 270 | 149 | 37.3 |
| Bulk density | 0.19 | 0.15 | 0.13 | 0.15 | 0.30 |
| Pore volume ($cm^3 g^{-1}$) | | | | | |
| ($D < 30$ nm) | 0.86 | 1.06 | 0.95 | 0.57 | 0.09 |
| ($D > 30$ nm) | 2.52 | 3.67 | n.d. | n.d. | 1.81 |
| Total | 3.38 | 4.73 | n.d. | n.d. | 1.90 |
| Mode pore diameter (nm) | | | | | |
| mesopore region | 20 | 16 | 19 | 28 | – |

[a] Glycothermal treatment conditions, 300 °C for 2 h.

these aluminas have potential for use as catalyst support.

## Acknowledgements

The authors wish to acknowledge Dr A. Nishino and Mr Y. Ono, Matsushita Electric Industrial Co., Ltd, for help with mercury porosimetry.

## References

1. D. L. TRIMM and A. STANISLAUS, *Appl. Catal.* **21** (1986) 215.
2. P. N. HO and S. W. WELLER, *Fuel Process. Technol.* **4** (1981) 21.
3. H. SHIMADA, M. KURITA, T. SATO, Y. YOSHIMURA, T. KAWAKAMI, S. YOSHITOMI and A. NISHIJIMA, *Bull. Chem. Soc. Jpn* **57** (1984) 2000.
4. W. C. VAN ZIJLL LANGHOUT, C. OUWERKERK and K. M. A. PRONK, *Oil & Gas J.* Dec. 1 (1980) 120.
5. R. K. OBERLANDER, in "Applied Industrial Catalysts", Vol. 3, edited by B. E. Leach (Academic Press, New York, 1984) p. 63.
6. B. C. LIPPENS and J. H. de BOER, *Acta Crystallogr.* **17** (1964) 1312.
7. S. J. WILSON, *Miner. Mag.* **43** (1979) 247.
8. *Idem, J. Solid State Chem.* **30** (1979) 247.
9. S. J. WILSON, J. D. C. McCONNELL and M. H. STACEY, *J. Mater. Sci.* **15** (1980) 3081.
10. S. J. WILSON and M. H. STACEY, *J. Colloid Interface Sci.* **82** (1981) 507.
11. D. BASMADJIAN, G. N. FULFORD, B. I. PARSONS and D. S. MONTGOMERY, *J. Catal.* **1** (1962) 547.
12. T. INUI, T. MIYAKE and Y. TAKEGAMI, *J. Jpn Petrol. Int.* **25** (1982) 242.
13. T. INUI, T. MIYAKE, K. FUKUDA and Y. TAKEGAMI, *Appl. Catal.* **6** (1983) 165.
14. M. INOUE, Y. KONDO and T. INUI, *Inorg. Chem.* **27** (1988) 215.
15. M. INOUE, H. KOMINAMI and T. INUI, *J. Chem. Soc. Faraday Trans.* (1991) 3331.
16. R. W. CRANSTON and F. A. INKLEY, *Adv. Catal.* **9** (1957) 143.
17. S. WINSTEIN, E. ALLERD, R. HECK and R. GLICK, *Tetrahedron* **3** (1958) 1.
18. J. H. de BOER, in "The Structure and Properties of Porous Materials", edited by D. H. Everett and F. S. Stone (Butterworth, London, 1958) p. 68.
19. B. C. LIPPENS, B. G. LINSEN and J. H. de BOER, *J. Catal.* **3** (1964) 32.
20. B. C. LIPPENS and J. H. de BOER, *ibid.* **4** (1965) 319.
21. J. H. de BOER and B. C. LIPPENS, *ibid.* **3** (1964) 38.
22. B. C. LIPPENS and J. H. de BOER, *ibid.* **3** (1964) 44.

*Received 7 January*
*and accepted 8 October 1993*